



**1,5-diaminotetrazole-4*N*-oxide (SYX-9): a new high-performing energetic material with a calculated detonation velocity over 10 km s<sup>-1</sup>**

Journal:	<i>Journal of Materials Chemistry A</i>
Manuscript ID	TA-ART-10-2021-009275.R1
Article Type:	Paper
Date Submitted by the Author:	27-Dec-2021
Complete List of Authors:	Yocca, Sebastian; Purdue University, Chemical Engineering Zeller, Matthias; Youngstown State University, Department of Chemistry Byrd, Edward; ARL, DEVCOM Piercey, Davin; Purdue University, Materials Engineering, Mechanical Engineering

## ARTICLE

# 1,5-diaminotetrazole-4*N*-oxide (SYX-9): a new high-performing energetic material with a calculated detonation velocity over 10 km s<sup>-1</sup> †

Received 00th January 20xx,  
Accepted 00th January 20xx

DOI: 10.1039/x0xx00000x

Sebastian R. Yocca,<sup>a,b,c</sup> Matthias Zeller,<sup>d</sup> Edward F. C. Byrd,<sup>e</sup> and Davin G. Piercey<sup>\*b,c,f</sup>

5-amino-1-benzyloxytetrazole was aminated with *O*-tosylhydroxylamine. The diaminobenzyloxytetrazolium intermediate was debenzylated to yield the highly energetic 1,5-diaminotetrazole-4*N*-oxide (SYX-9). The molecule underwent both chemical and energetic characterization, including <sup>15</sup>N NMR spectroscopy and single-crystal X-ray crystallography, which reported a 1.820 g cm<sup>-3</sup> ambient temperature density. Theoretical energetic performances were determined by a combined experimental-computational method using calculated heats of formation and experimental room temperature densities. SYX-9 was calculated to have an exciting detonation velocity of 10,000 m s<sup>-1</sup>, making this energetic tetrazole molecule one of the few energetic materials reaching this high performance milestone. This material was found to be very sensitive to mechanical and thermal stimuli.

## Introduction

Energetic material research strives to understand and improve the performance, versatility, and sustainability for both novel and legacy energetic materials. Investigations into a unique energetic system provide a greater understanding of a material's physical characteristics, which can guide research toward improved energetic material. Additionally, detonation performance advancements are desired by both military and civilian sectors because of the need for greater explosive or propellant force.<sup>1,2</sup> Development of energetic materials with various levels of sensitivity are also promoted, as some applications require extremely sensitive or insensitive material.<sup>3,4</sup> Recently, the sustainability and environmental impact of energetic material production and detonation have been factored in as well.<sup>5,6</sup>

Modern energetic material design relies on two fundamental principles. First, both a fuel and oxidizer component should exist within an energetic material. This strategy is exemplified by popular explosives 1,3,5-trinitro-1,3,5-triazinane (RDX) and 1,3,5,7-tetranitro-1,3,5,7-

tetrazocane (HMX), which feature a carbon ring fuel source and substituent nitro group oxidizers. Secondly, a novel energetic material should exhibit high heat of formation. This is achieved by either incorporation of a highly strained ring or cage backbone like octanitrocubane (ONC)<sup>7</sup> or via high-nitrogen content compounds.<sup>8</sup> Nitrogen-rich molecules often feature large energy differences between pre- and post-decomposition products, which is realized as explosive energy. Upon detonation, nitrogen atoms often form N<sub>2</sub> gas, which is both non-toxic and has a zero heat of formation by definition, thus maximizing the released explosive force. However, increasing a heat of formation and detonative performance generally comes at the cost of stability, making many high-performing energetic materials excessively sensitive.<sup>9</sup> Therefore, an interplay between performance and stability exists, and it is necessary to create new energetic materials to optimize both.

Nitrogen-rich 5-membered heterocycles, such as triazoles,<sup>10,11</sup> tetrazoles,<sup>12,13</sup> and pentazoles<sup>6,14</sup> have been recently considered energetically due to their favorable high heat of formations. These nitrogen-containing rings are not as stable as similar carbon-based heterocycles due to the free electron pair attached to each nitrogen. The free electron pairs have the capability to enter adjacent σ\* orbitals, thus destabilizing and decomposing the ring's structure.<sup>15</sup> Unfortunately, this means that higher nitrogen-content rings may feature favorable heats of formation but also decreased stabilities. For example, the pentazole ring contains the highest heat of formation of the possible 5-membered nitrogen heterocycles but is of low thermal stability.<sup>16</sup> Attaching substituents to heterocyclic rings is a popular method for stabilizing the unstable. In fact, it is possible to both increase stability and energetic performance with the correct explosophoric group additions. 1,2,3,4-tetrazines, for example, are mostly unstable under ambient conditions, whereas

<sup>a</sup> Department of Chemical Engineering, Purdue University, 480 Stadium Mall Drive, West Lafayette, IN, 47906, USA.

<sup>b</sup> Department of Materials Engineering, Purdue University, 205 Gates Road, West Lafayette, IN, 47906, USA.

<sup>c</sup> Purdue Energetics Research Center, Purdue University, 205 Gates Road, West Lafayette, IN, 47906, USA.

<sup>d</sup> Department of Chemistry, Purdue University, 560 Oval Drive, West Lafayette, IN, 47906, USA.

<sup>e</sup> Detonation Sciences & Modeling Branch, CCDC U. S. Army Research Laboratory, Aberdeen Proving Ground, MD, 21005, USA.

<sup>f</sup> Department of Mechanical Engineering, Purdue University, 585 Purdue Mall, West Lafayette, IN, 47906, USA.

† Electronic Supplementary Information (ESI) available: (1) IR, NMR, and DSC/TGA materials (2) X-ray diffraction. CCDC 2118464-2118466. For ESI and crystallographic data in CIF or other electronic format see DOI: 10.1039/x0xx00000x

disubstituted 1,2,3,4-tetrazine-1,3-dioxides are often thermally stable to temperatures over 200 °C.<sup>17</sup>

An important parameter for any novel energetic material is its detonation velocity, which measures how fast the detonation shock wave propagates within a material. Traditional explosives RDX (8,983 m s<sup>-1</sup>), HMX (9,221 m s<sup>-1</sup>), and CL-20 (9,455 m s<sup>-1</sup>) provide performance benchmarks for comparing new and old energetic materials.<sup>18</sup> Only a few energetic materials feature calculated detonation velocities over 10,000 m s<sup>-1</sup>, including ONC<sup>7</sup> at 10,100 m s<sup>-1</sup> and 4,4'-dinitro-3,3'-diazonofuroxan (DDF)<sup>19</sup> at 10,000 m s<sup>-1</sup>. These explosives represent the current maximum frontier of detonative performance, however feature long and costly syntheses, thus making scalability unfeasible. Computational studies have shown that tetrazole oxides could achieve better energetic performances than both ONC and DDF.<sup>20</sup> For example, DFT calculations on theoretical compound 1-amino-5-nitrotetrazole-4*N*-oxide featured an unprecedented calculated detonation performance of 10,740 m s<sup>-1</sup> alongside a large calculated 2.202 g cm<sup>-3</sup> density.<sup>21</sup> Therefore, there exists a high incentive to synthesize novel energetic tetrazole oxide materials, given they could push the limits of performance for CHNO energetic materials.

Few neutral tetrazole oxide materials, however, have been successfully synthesized in the energetics community. Multiple negatively charged tetrazolate oxides have been created, such as the 5-nitrotetrazolate-2*N*-oxide, 5-azidotetrazolate-2*N*-oxide, and 5,5'-bistetrazole-1,1'-diolate anions.<sup>22,23</sup> When compared to their parent "non-oxidized" tetrazoles, the tetrazolate oxides have generally showed improved mechanical stability but worse thermal stability. The most promising tetrazolate oxide energetic material is the dihydroxylammonium 5,5'-bistetrazole-1,1'-diolate salt (TKX-50), which features excellent density (1.877 g cm<sup>-3</sup>), detonation velocity (9,698 m s<sup>-1</sup>), and detonation pressure (424 kbar) while being relatively insensitive to impact (20 J) and frictional stimulus (120 N).<sup>18</sup> Examples of neutral tetrazole oxides are very limited in literature. In 2010, Harel and Rosen achieved a variety of nonenergetic tetrazole-2*N*-oxides disubstituted with aryl or alkyl groups.<sup>24</sup> An energetic neutral tetrazole *N*-oxide material came from Chavez et al., who synthesized a tetrazolo-1,2,4,5-tetrazine oxide, which was then oxidized further to incorporate a 2*N*-oxide on the tetrazole ring.<sup>25</sup> Both groups used hypofluorous acid (HOF) as their oxidant, which requires the use of fluorine gas and often produces low yields of product. Additionally, relevant energetic substituents such as amino, azo, and azido groups may be oxidized or destroyed under HOF's strong oxidizing conditions. Alternatively, one could suggest using a weaker oxidizing agent on a tetrazole heterocycle like Oxone® however, this oxidant, while it does work on anionic tetrazoles, is not strong enough to oxidize a neutral tetrazole ring. A novel oxide introduction method had to be developed in order to synthesize potentially high-performing neutral tetrazole oxides.

In this work we synthesized and characterized highly energetic 1,5-diaminotetrazole-4*N*-oxide (**SYX-9**) via a new, indirect method of neutral tetrazole *N*-oxide formation that

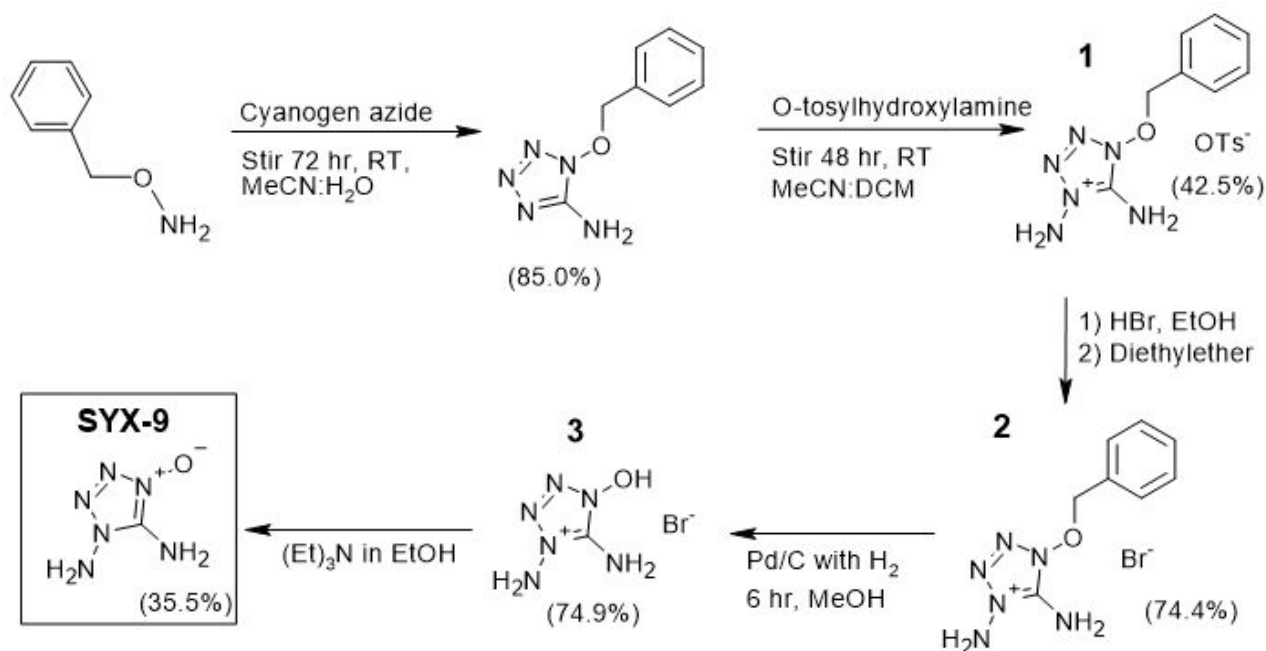
avoids direct oxidation of the parent heterocycle. **SYX-9** could be considered an oxidized form of 1,5-diaminotetrazole (DAT), which has found extensive use in various energetic material syntheses.<sup>26</sup> Additionally, **SYX-9** has not been previously reported in literature. In fact, only one other energetic material (1-amino-1,2,3-triazole-3*N*-oxide)<sup>27</sup> has been reported that contains both an *N*-amine and *N*-oxide on the same heterocycle. **SYX-9** is the first neutrally charged tetrazole oxide of such kind. The molecule has been chemically characterized by <sup>1</sup>H NMR, <sup>13</sup>C NMR, <sup>15</sup>N NMR, IR spectroscopy, and X-ray Crystallography. **SYX-9** has been energetically characterized by its impact and friction sensitivity tests, as well as its thermal decomposition point. Theoretical detonative properties were calculated based on its heat of formation and observed crystal density at room temperature. The high nitrogen content, large density, and excellent calculated detonation velocity of **SYX-9** make it of high interest for the scientific and energetics community and offers a route that exemplifies a new method of creating high energy molecules.

## Results and discussion

**Synthesis.** The synthesis of the **SYX-9** is depicted in Scheme 1. 1-benzyloxy-5-aminotetrazole was synthesized via a scaled down literature method from Joo et al.,<sup>28</sup> in which an acetonitrile solution of cyanogen azide is combined with an aqueous solution of *O*-benzylhydroxylamine and stirred for 72 hours. After mixing, the solution was evaporated under an air-line to a crude yellow solid, washed with cold water and acetonitrile to yield pure 1-benzyloxy-5-aminotetrazole.

Ethyl-*O*-(*p*-tolylsulphonyl)-acetohydroximate was freshly prepared via literature methods<sup>29</sup> and yielded the aminating agent, *O*-tosylhydroxylamine, by stirring in 60% perchloric acid for two hours at room temperature.<sup>10</sup> The tetrazole benzyl ether was aminated by combining the *O*-tosylhydroxylamine in a 1:1 acetonitrile: dichloromethane solution and stirred for 18 hours. An off-white solid precipitated out of solution and was filtered and dried to yield pure 4-benzyloxy-1,5-diaminotetrazolium tosylate (**1**). The tosylate anion was exchanged for a bromide anion by dissolving in minimal ethanol and adding a molar excess of hydrobromic acid. An excess of diethylether was added to induce precipitation of pure, white 4-benzyloxy-1,5-diaminotetrazolium bromide (**2**).

The benzyl group was removed by dissolving dried **2** in anhydrous methanol with 10% (w/w) Pd/C catalyst in suspension. H<sub>2</sub> gas was bubbled through the solution for 6 hr. The H<sub>2</sub> gas was produced from stirring zinc metal and dilute sulfuric acid together. After the hydrogenation reaction, the orange solution was filtered through Celite® to remove unwanted catalyst. The solution was dried under a stream of air to yield a crude orange solid containing 1,5-diamino-4-hydroxytetrazolium bromide (**3**). The solid was then redissolved in anhydrous ethanol and neutralized to a pH of 8 using dilute triethylamine in ethanol. The neutralized solution was evaporated partially and grey precipitate was collected via vacuum filtration, washed with cold ethanol and diethylether, and dried to yield **SYX-9**.



Scheme 1 Complete synthesis of 1,5-diaminotetrazole-4*N*-oxide (**SYX-9**).

**Spectroscopy.** The **SYX-9** compound and its precursors were characterized with multinuclear <sup>1</sup>H, <sup>13</sup>C, and <sup>15</sup>N NMR spectroscopy. **SYX-9** contained two unique hydrogen resonances at 6.7 ppm and 7.2 ppm, which represent the *N*-amine and *C*-amine, respectively. When compared to 1,5-diaminotetrazole, the inclusion of the 4*N*-oxide on the tetrazole ring shifted the *N*-amine peak by 0.1 ppm and the *C*-amine peak by 0.3 ppm.<sup>30</sup>

For <sup>13</sup>C NMR spectroscopy, **SYX-9** featured a single carbon resonance at 139.4 ppm. For comparison, the same carbon for the 1-benzyl-5-aminotetrazole and the intermediate salts **1**, **2**, and **3** resonated at 149.9, 146.0, 146.0, and 143.0 ppm, respectively. The ortho position *N*-amination shielded the carbon by 3.9 ppm. The debenzoylation process and the formation of the hydroxyl group shielded the carbon atom an additional 3.0 ppm. Lastly, the deprotonation of the hydroxyl group to yield **SYX-9** shielded the carbon an additional 3.6 ppm.

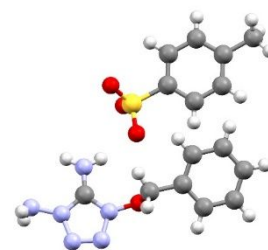
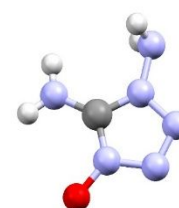
<sup>15</sup>N NMR was performed both on precursor 1-benzyl-5-aminotetrazole and **SYX-9**. The precursor featured 5 differentiable nitrogen atoms: one amine and four azole. The amine nitrogen resonated at -335.9 ppm and the ring nitrogen atoms at -134.8 (N1), -94.9 (N4), -31.5 (N2), and -6.4 (N3) ppm. **SYX-9** displayed 2 amine nitrogen resonances at -334.8 (*C*-amine) and -306.5 (*N*-amine) ppm. Its ring nitrogen atoms resonated at -171.4 (N4), -133.3 (N1), -54.2 (N3), -28.5 (N2) ppm. The <sup>15</sup>N NMR data clearly shows how the amine group added electron density to the ring. **SYX-9** N2, N3, N4 azole nitrogen resonances were more shielded (electron denser) when compared to the precursor. This is exemplified by the N4 peak, which featured an upfield shift of 76.5 ppm after *N*-amination. Only a deshielding effect of 1.9 ppm was observed on the N1 zwitterionic nitrogen. Unfortunately, intermediates **1**, **2**, and **3** were unable to be analyzed because of their instability in DMSO-*d*<sub>6</sub>.

**Single Crystal X-ray Analysis.** Single crystals of **1**, **3**, and **SYX-9** were analyzed. Each crystal was coated with a trace of Fomblin oil and was transferred to the goniometer head of a Bruker Quest diffractometer. Compound **1**'s diffractometer had a fixed chi angle, a Mo K $\alpha$  wavelength ( $\lambda = 0.71073 \text{ \AA}$ ) sealed tube fine focus X-ray tube, single crystal curved graphite incident beam monochromator, and a Photon II area detector. Compounds **3** and **SYX-9** used a diffractometer with kappa geometry, a Cu K $\alpha$  wavelength ( $\lambda = 1.54178 \text{ \AA}$ ) I- $\mu$ -S microsource X-ray tube, laterally graded multilayer (Goebel) mirror for monochromatization, and a Photon III C14 area detector. Both diffractometers were equipped with an Oxford Cryosystems low temperature device and examination and data collection were performed at 150 K and ambient temperature. Data were collected, reflections were indexed and processed, and the files scaled and corrected for absorption using APEX3<sup>31</sup> and SADABS.<sup>32</sup> The space groups were assigned using XPREP within the SHELXTL suite of programs<sup>33,34</sup> and solved by direct methods using ShelXS<sup>34</sup> and refined by full matrix least squares against F<sup>2</sup> with all reflections using ShelXL2018<sup>35</sup> using the graphical interface ShelXL.<sup>36</sup> H atoms attached to carbon and nitrogen atoms as well as hydroxyl hydrogens were positioned geometrically and constrained to ride on their parent atoms. C-H bond distances were constrained to 0.95  $\text{\AA}$  for aromatic and alkene C-H and to 0.98  $\text{\AA}$  for CH<sub>3</sub> moieties, respectively. Amine H atom positions were refined. The crystallographic data, structure refinement details, and densities of compounds **1**, **3**, and **SYX-9** at 150 K are reported in Table 1.

All analyzed crystals were colorless. Intermediate tosylate salt **1** (Figure 1) was crystallized via slow ether diffusion into methanol as plates in a triclinic system with a *P*-1 space group and 2 formula units in each unit cell. At ambient temperature, salt **1** exhibited a density of 1.361 g cm<sup>-3</sup>. Rod-shaped **3**

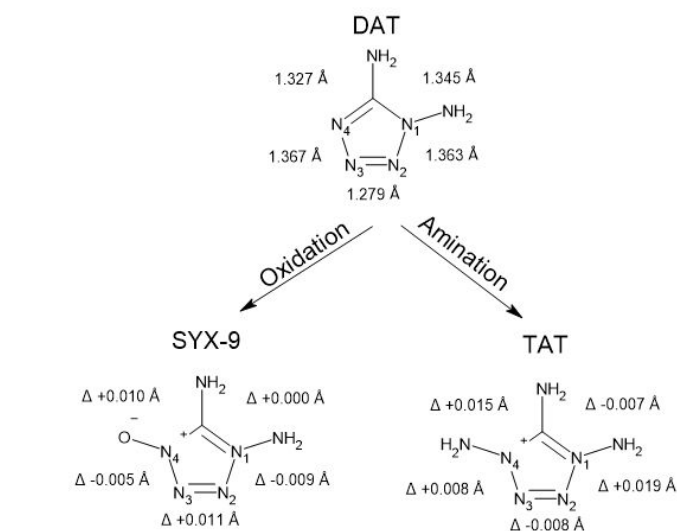
**Table 1.** Crystallographic data and structure refinement details for compounds **1**, **3**, **SYX-9**.

	<b>1</b>	<b>3</b>	<b>SYX-9</b>
Formula	C <sub>9</sub> H <sub>15</sub> N <sub>7</sub> SO <sub>4</sub>	(CH <sub>4.5</sub> N <sub>6</sub> O) <sub>2</sub> Br	CH <sub>4</sub> N <sub>6</sub> O
FW [g mol <sup>-1</sup> ]	378.41	313.12	116.10
Crystal system	Triclinic	Monoclinic	Monoclinic
Space Group	<i>P</i> -1	<i>P</i> 2 <sub>1</sub> / <i>c</i>	<i>P</i> 2 <sub>1</sub> / <i>c</i>
<i>a</i> [Å]	7.6351 (2)	8.3967 (5)	6.0034 (4)
<i>b</i> [Å]	8.2212 (3)	5.6497 (4)	14.4146 (9)
<i>c</i> [Å]	16.2653 (5)	11.8522 (8)	5.2071 (3)
$\alpha$ [°]	98.0291 (14)	90	90
$\beta$ [°]	98.6583 (13)	100.990 (3)	112.186 (2)
$\gamma$ [°]	113.9202 (13)	90	90
<i>V</i> [Å <sup>3</sup> ]	899.60	551.94	417.24
<i>Z</i>	2	2	4
$\rho$ [g cm <sup>-3</sup> ]	1.397	1.884	1.848
<i>T</i> [K]	150	150	150
Crystal shape	Plate	Rod	Block
Color	Colorless	Colorless	Colorless
Crystal size [mm]	0.04 x 0.14 x 0.44	0.09 x 0.11 x 0.41	0.19 x 0.18 x 0.13
<i>R</i> <sub>1</sub>	0.0392	0.0247	0.0383
<i>wR</i> <sub>2</sub>	0.1035	0.0550	0.0924
<i>S</i>	1.070	1.000	1.077
No. of reflections	3764	2113	1592
Parameters	248	94	85
Restraints	0	1	0
CCDC	2118464	2118465	2118466

**Fig. 1** Molecular unit of 4-benzoyloxy-1,5-diaminotetrazolium tosylate (**1**). Ellipsoids are drawn at the 50% probability level.**Fig. 2** Molecular unit of 4-hydroxyl-1,5-diaminotetrazolium bromide (**3**). Ellipsoids are drawn at the 50% probability level.**Fig. 3** Molecular unit of 1,5-diaminotetrazole-4*N*-oxide (**SYX-9**). Ellipsoids are drawn at the 50% probability level.

crystallized from slow ether diffusion into methanol as a hemihydrobromic acid salt in a monoclinic system as a *P*2<sub>1</sub>/*c* space group with 2 formula units per unit cell. The tetrazolium bromide intermediate **3** (Figure 2) featured a larger 1.860 g cm<sup>-3</sup> density at room temperature because of the removal of the benzyl protecting group and the replacement of the tosylate group with a heavy bromide anion. Lastly, **SYX-9** (Figure 3) crystallized in a monoclinic system with a *P*2<sub>1</sub>/*c* space group with 4 formula units per unit cell. Crystallization of **SYX-9** was achieved from both ethanol evaporation under an air-line and evaporation of DMSO to atmosphere. **SYX-9** crystallized as a block, and featured a density of 1.848 g cm<sup>-3</sup> at 150 K and 1.820 g cm<sup>-3</sup> at room temperature. **SYX-9**'s density was slightly larger than traditional benchmark RDX (1.81 g cm<sup>-3</sup>)<sup>18</sup>, which highlights the importance of this novel energetic compound. Other 10 km s<sup>-1</sup> energetics like octanitrocubane (ONC)<sup>7</sup> and 4,4'-dinitro-3,3'-diazanofuroxan (DDF)<sup>19</sup> feature much larger densities than **SYX-9** of 2.03 and 2.0 g cm<sup>-3</sup>, respectively.

X-ray crystallography also allows an insightful comparison of bond lengths among the 1,4,5-triaminotetrazolium cation (TAT), 1,5-diaminotetrazole (DAT), and compounds **1**, **3**, and **SYX-9**. Crystallographic data for DAT<sup>37</sup> and TAT NO<sub>3</sub><sup>29</sup> (Figure 4) were taken from CCDC CIF files 159997 and 896691. Corresponding bond lengths are displayed in Table 2. For consistency purposes, N1 represents the original *N*-amine nitrogen for all compounds as illustrated in Figure 4.

**Fig. 4** Comparison of bond lengths of tetrazole moieties: DAT, **SYX-9**, and TAT. The oxidation of DAT to **SYX-9** strengthened the weakest bonds, while the amination of DAT to TAT weakened the weakest bonds.

The N – O bond becomes shorter going from benzyl (1.360 Å) to hydroxyl (1.339 Å) to oxide (1.318 Å). This showed the bond's strengthening as the compound exhibited more zwitterionic behavior. Also, **SYX-9**'s N4-oxide bond length is 0.072 Å shorter than the TAT N4-amine bond, which contributed greatly to the **SYX-9**'s superior experimental density.

A comparison to other *N*-oxide tetrazole compounds is also warranted. Klapötke et al. synthesized the 5-nitrotetrazolate-

**Table 2.** Bond lengths of comparable tetrazole and tetrazolium moieties (Å).

	<b>1</b>	<b>3</b>	<b>SYX-9</b>	DAT	TATNO <sub>3</sub>
N1 – N2	1.370(2)	1.365(2)	1.354(2)	1.363(1)	1.381(4)
N2 – N3	1.277(2)	1.283(2)	1.290(1)	1.279(1)	1.271(3)
N3 – N4	1.359(3)	1.353(2)	1.362(2)	1.367(1)	1.375(3)
C – N4	1.342(2)	1.336(2)	1.337(1)	1.327(1)	1.342(3)
C – N1	1.345(3)	1.335(2)	1.345(1)	1.345(1)	1.338(3)
N1 – NH <sub>2</sub>	1.387(2)	1.389(2)	1.388(1)	1.383(1)	1.385(3)
C – NH <sub>2</sub>	1.304(3)	1.311(2)	1.324(2)	1.334(1)	1.308(4)
N4 – NH <sub>2</sub>	-	-	-	-	1.390(4)
N4 – O	1.360(2)	1.339(2)	1.318(1)	-	-

2*N*-oxide anion.<sup>22</sup> This tetrazolate oxide anion had an average 2*N*-oxide bond length measuring 1.295 Å. Chavez et al. synthesized a neutrally charged tetrazolo-tetrazine 2*N*-oxide compound and achieved a crystal structure.<sup>25</sup> The tetrazolo N – O bond length measured at 1.260 Å. Both the tetrazolate and tetrazole 2*N*-oxide feature shorter and stronger N – O bonds than **SYX-9**'s 4*N*-oxide bond (1.318 Å).

The C – NH<sub>2</sub> bond length increased as the N4-oxide became less protected going from **1** (1.304 Å) to **3** (1.311 Å) to **SYX-9** (1.324 Å). Structurally related TAT featured a shorter and stronger C – NH<sub>2</sub> (1.308 Å) bond than **SYX-9** (1.324 Å), which could be explained by the replacement of the electron donating oxide group with the more electron withdrawing amine group. The original N1 – NH<sub>2</sub> bond length is mostly unaffected by the presence of an oxide or an amine group on the N4 position (TAT and **SYX-9** bond lengths remain within .01 Å from DAT).

The tetrazole perimeter of the non-oxidized DAT's ring measures at 6.681 Å. The addition of the N4-oxide group slightly increased the perimeter to 6.688 Å, while the N4-amine group greatly increased the perimeter to 6.707 Å. Ring stability is directly related to the ring's aromaticity, with shorter perimeters being more aromatic and stable. Therefore, the TAT ring's larger perimeter resulted in a decrease in aromaticity and stability, which matches the lower observed thermal stabilities of TAT salts. **SYX-9** and DAT exhibited more similar perimeters, and thus more similar, higher stabilities.

By comparing the individual ring bond lengths of DAT to both **SYX-9** and TAT, one can show how *N*-oxide and *N*-amino groups affect sensitivity. By adding the N4 substituent to DAT, the tetrazole C-N bond lengths grew by a similar average amount for both **SYX-9** (0.005 Å) and TAT (0.004 Å). Interestingly, the longest bond lengths and thus weakest bond strengths of DAT's ring were the N1 – N2 (1.363 Å) and N3 – N4 (1.367 Å) linkages. The N4-oxidation of DAT to **SYX-9** decreased both the N1 – N2 (1.362 Å) and N3 – N4 (1.354 Å) lengths, indicating greater bond strength. Additionally, **SYX-9** featured a longer and weaker N2 – N3 bond (1.290 Å) than the corresponding DAT N2 – N3 bond (1.279 Å). However, **SYX-9**'s N2 – N3 bond remained stronger than the rest of the tetrazole ring bonds due to its overlapping resonance structures, so the N2 – N3 weakening has little effect on the stability of the molecule. In summary, the *N*-oxide strengthened the most unstable connections within the tetrazole ring at the expense of the most stable bond within the ring. This data directly supports the *N*-oxide's potential ability to be incorporated into a

tetrazole ring without adverse effects on the aromaticity of the system.

In contrast, the amination of DAT to TAT had the opposing effect on its ring stability. The N4-amine strengthened the already strong N2 – N3 bond (1.271 Å), while both the N1 – N2 (1.381 Å) and N3 – N4 (1.375 Å) linkages became weaker. TAT nitrate is reported to decompose at a lower temperature (78 °C). This decreased thermal stability can be attributed to the DAT amination's weakening of the N1 – N2 and N3 – N4 bonds making it easier for N2 and N3 to form N<sub>2</sub> gas.

Complete crystallographic data, in CIF format, have been deposited with the Cambridge Crystallographic Data Centre. CCDC 2118464-2118466 contain the supplementary crystallographic data for this paper. These data can be obtained free of charge from The Cambridge Crystallographic Data Centre via [www.ccdc.cam.ac.uk/data\\_request/cif](http://www.ccdc.cam.ac.uk/data_request/cif).

**Physical Characteristics.** The thermal behaviours of salts **1** and **2** and **SYX-9** were investigated by either differential scanning calorimetry (DSC) or thermogravimetric analysis (TGA). Heating rates for both methods were 5 °C min<sup>-1</sup>. **SYX-9** underwent thermal decomposition starting at 137 °C. This thermal limit is greater than fellow 10 km s<sup>-1</sup> detonation velocity explosive DDF (128 °C)<sup>38</sup>, but inferior to ONC (200 °C).<sup>39</sup> At 141 °C, the molecule sharply exploded. According to Lesnikovich et al., 1,5-diaminotetrazole decomposes at 197 °C.<sup>40</sup> This shows that the addition of the *N*-oxide to the DAT ring decreased the thermal decomposition point by 60 °C. Unfortunately, **SYX-9**'s low thermal stability severely limits its possible application as an explosive. RDX has a decomposition temperature of 210 °C.<sup>18</sup>

Interestingly, precursor salts **1** (88 °C) and **2** (95 °C) were more prone to thermal decomposition than zwitterionic **SYX-9**. The precursors' high sensitivities to elevated temperatures were attributed to the tetrazolium cations' extra amine group, which forced a positive charge throughout the ring and a decrease in aromatic behavior, as evidenced by the previous bond length discussion.

The precursors **1**, **2** and **3** were also shown to decompose if left in certain solvents over time, like water and DMSO. Therefore, weak nucleophiles can be expected to further destabilize the tetrazolium ring and cause decomposition. Hence, why all solvents used after formation of the tetrazolium were made anhydrous if possible. **SYX-9** was more resistant to decomposing than its precursors. However, **SYX-9** had shown to decompose in DMSO over the timespan of a few hours. It was determined that **SYX-9** was partially soluble in dichloromethane, dimethylformamide, and methanol while completely insoluble in ether and acetonitrile.

**Mechanical Sensitivity.** Compound **SYX-9** underwent mechanical sensitivity testing, and the results are found in Table 3. Impact sensitivity was performed according to STANAG 4489 and modified according to instruction<sup>41</sup> on an OZM drophammer by BAM method.<sup>42</sup> Friction sensitivity was carried out in accordance with STANAG 4487<sup>43</sup> and modified according to instruction<sup>44</sup> using a BAM friction tester.

## ARTICLE

**Table 3.** Energetic properties and calculated detonation parameters for **SYX-9** and related explosives.

	<b>SYX-9</b>	RDX <sup>18</sup>	HMX <sup>18</sup>	CL-20 <sup>18</sup>	TKX-50 <sup>18</sup>	TAT NO <sub>3</sub> <sup>29</sup>
Formula	CH <sub>4</sub> N <sub>6</sub> O	C <sub>3</sub> H <sub>6</sub> N <sub>6</sub> O <sub>6</sub>	C <sub>4</sub> H <sub>8</sub> N <sub>8</sub> O <sub>8</sub>	C <sub>6</sub> H <sub>6</sub> N <sub>12</sub> O <sub>12</sub>	C <sub>2</sub> H <sub>8</sub> N <sub>10</sub> O <sub>4</sub>	CH <sub>6</sub> N <sub>8</sub> O <sub>3</sub>
FW (g mol <sup>-1</sup> )	116.08	222.12	296.16	438.19	236.15	178.11
Ω <sup>a</sup> (%)	-41.4	-21.6	-21.6	-11.0	-27.1	-18.0
T <sub>d</sub> <sup>b</sup> (°C)	137	210	279	215	221	78
ρ <sup>c</sup> (g cm <sup>-3</sup> )	1.820	1.81	1.90	2.08	1.877	1.663
ρ <sup>calc d</sup> (g cm <sup>-3</sup> )	1.730	-	-	-	-	-
Δ <sub>f</sub> H <sub>m</sub> <sup>o</sup> (kJ mol <sup>-1</sup> )	365.9	86.3	116.1	918.7	446.6	1743.2
IS <sup>f</sup> (J)	< 1	7.5	7	4	20	2
FS <sup>g</sup> (N)	30	120	112	48	120	5
Calculated Values by EXPLO5						
Δ <sub>Ex</sub> U <sup>o h</sup> (kJ kg <sup>-1</sup> )	6362	6190	6185	6406	6025	5745
T <sub>det</sub> <sup>i</sup> (K)	3269	4232	4185	4616	3954	4006
P <sub>cl</sub> <sup>j</sup> (kbar)	386	380	415	467	424	311
V <sub>det</sub> <sup>k</sup> (m s <sup>-1</sup> )	10000	8983	9221	9455	9698	8879
I <sub>sp</sub> <sup>l</sup> (s)	254	258	258	251	261	-

<sup>a</sup>Oxygen balance. <sup>b</sup>Temperature decomposition. <sup>c</sup>Density from X-ray diffraction (25°C). <sup>d</sup>Calculated density. <sup>e</sup>Calculated molar enthalpy of formation. <sup>f</sup>Impact sensitivity. <sup>g</sup>Friction sensitivity. <sup>h</sup>Total energy of detonation. <sup>i</sup>Detonation temperature. <sup>j</sup>Detonation pressure. <sup>k</sup>Detonation velocity. <sup>l</sup>Specific impulse.

**SYX-9** was sensitive to both impact (< 1 J) and friction (30 N) stimuli. Frictional stress triggered **SYX-9**, which resulted in a loud snapping noise. Impact stress caused **SYX-9** to rapidly decompose into gas. **SYX-9** was more sensitive than other popular secondary explosives, like RDX (7.5 J, 120 N) and HMX (7 J, 112 N). Unfortunately, the elevated sensitivity limits **SYX-9**'s possible application to future explosives.

**Detonation Parameters.** The theoretical energetic performance of **SYX-9** was calculated. Intermediates **1**, **2**, and **3** were not analyzed because of their unenergetic tosylate and bromide anions. All detonation characteristics were calculated using theoretical heat of formation and experimental X-ray crystallography room temperature density. The calculated energetic properties of **SYX-9** are shown in Table 3 alongside previously mentioned explosives.

The method of Byrd and Rice (based on properties of individual energetic compounds derived from quantum mechanics), provided the heats of formation<sup>45</sup> and theoretical density<sup>46,47</sup> of **SYX-9**. The Gaussian09 program package<sup>48</sup> and the B3LYP spin-restricted Kohn-Sham density functional theory (KS-DFT)<sup>49–52</sup> with the 6-31G\*\* and 6-31 ++G(3df,2p) Pople Gaussian basis set<sup>53–55</sup>, were used to determine gas phase geometries of **SYX-9**. The heat of formation for **SYX-9** was calculated to be 365.9 kJ mol<sup>-1</sup>, which surpasses heats of formations of both RDX and HMX. The EXPLO5 V6.05.02

software package<sup>56,57</sup> provided the detonation performance data from the calculated heats of formation based on observed X-ray diffraction crystal densities at ambient temperature.

**SYX-9** achieved excellent calculated detonative parameters. The EXPLO5 program calculated the detonation velocity of **SYX-9** to be 10,000 m s<sup>-1</sup> with a detonation pressure of 386 kbar. **SYX-9** surpassed the detonation velocity for modern explosives including RDX, HMX, CL-20 and TKX-50. In fact, the calculated detonation velocity of **SYX-9** was over 10% larger than the velocity for RDX (8,983 m s<sup>-1</sup>). The 10,000 m s<sup>-1</sup> calculated detonation velocity is significant because few previously synthesized organic energetic materials in existence have reached this milestone. The calculated detonation pressure surpassed only RDX. This is attributed to the **SYX-9**'s lower density, which is closely linked to an energetic molecule's detonation pressure.<sup>58</sup>

Additionally, **SYX-9** was theoretically calculated as a possible explosive filler for novel propellant compositions. Pure **SYX-9** showed a promising calculated specific impulse of 254 s, which is less than current propellant explosives RDX, HMX, and CL-20. Klapötke and Sueska have recently calculated specific impulse for a variety of composite mixtures containing 10% glycidyl azide polymer (GAP), 15% nitroglycerin (NG), 18% aluminium, and a variable percentage of oxidizer ammonium perchlorate and select energetic material (Table 4).<sup>59</sup> The percentages of ammonium perchlorate and explosive were set to achieve a

**Table 4.** Calculated specific impulses for various explosive propellant composites for popular secondary explosives and **SYX-9** using Klapötke and Suceska's method.<sup>59</sup>

	HMX	CL-20	TKX-50	<b>SYX-9</b>
Composite Formulation	57% GAP, NG, Al	57% GAP, NG, Al	57% GAP, NG, Al	57% GAP, NG, Al
	45% HMX, 12% AP	54% CL-20, 3% AP	41% TKX-50, 16% AP	32% <b>SYX-9</b> , 25% AP
Specific impulse (s)	274	275	278	275

-33% oxygen balance, which corresponds to modern propellant formations. Using EXPLO5 software, Klapötke and Suceska calculated the specific impulse for HMX, CL-20, and TKX-50 composites to be 274 s, 275 s, and 278 s, respectively. A **SYX-9** composite material using Klapötke and Suceska's conditions (25% ammonium perchlorate, 32% **SYX-9**) achieved a competitive 275 s calculated specific impulse. However, **SYX-9**'s increased sensitivity again limits its practical application.

## Conclusions

In summary, a novel 1,5-diaminotetrazole-4*N*-oxide molecule (**SYX-9**) was created and fully characterized chemically and energetically. This was achieved by reacting the strong aminating agent *O*-tosylhydroxylamine with benzyloxyaminotetrazole to yield the benzyloxy diaminotetrazolium intermediate. Via a Pd/C hydrogenation technique, the benzyl group was removed to yield the hydroxyl diaminotetrazolium salt. Lastly, the ethanol insoluble **SYX-9** was isolated by neutralizing with an organic base. The theoretical energetic performance of **SYX-9** is exciting, boasting a calculated detonation velocity (10,000 m s<sup>-1</sup>) that exceeds RDX, HMX, and CL-20. This can be attributed to the molecule's high nitrogen content and comparable density. **SYX-9** is quite sensitive (IS: < 1 J, FS: 30 N, T<sub>dec</sub> = 137 °C), however not as thermally sensitive as structurally-related triaminotetrazolium salts due to the stabilizing effect of its ring's *N*-oxide. Possibly most exciting is that the *C*- and *N*- amines of **SYX-9** offer further simple modification opportunities for additional energetic zing. **SYX-9** is limited, however, in its real-world application by its low thermal stability and sensitive nature.

## Experimental

**General.** All reagents and solvents were used as received unless otherwise specified (Sigma-Aldrich, Fluka, Acros Organics, Fisher Scientific Co LLC). Decomposition temperatures were acquired using a TA Instruments SDT Q600 TGA/DSC using heating rates of 5 °C min<sup>-1</sup>. Salt characterization using Elemental Analysis was conducted using an Elementar Vario EL cube. **SYX-9** was too sensitive for elemental analysis measurement. All NMR (<sup>1</sup>H, <sup>13</sup>C, <sup>15</sup>N) spectroscopy was collected with a Bruker AV-III-500-HD (5mm BBFO Cryoprobe Prodigy) Avance DRX NMR spectrometer. All chemical shifts for <sup>1</sup>H and <sup>13</sup>C spectra are relative to TMS. <sup>15</sup>N shifts are reported relative to nitromethane. Infrared spectra were measured with a

PerkinElmer Spectrum Two FT-IR spectrometer. Transmittance values are described as "strong" (s), "medium" (m) and "weak" (w). The BAM (Bundesanstalt für Materialforschung) friction tester from Reichel & Partner GmbH and the OZM BAM Fall Hammer BFH-10 were used to acquire sensitivity data.

**WARNING.** **SYX-9** is considered an energetic material that could be detonated by various stimuli. Additionally, the cyanogen azide intermediate is an extremely sensitive explosive and could detonate if dry. During our experiments, we did not encounter issues while handling the materials. However, personal protective equipment (face shield, body armor, Kevlar gloves, grounded equipment) should be used when appropriate.

### 1-benzyloxy-5-aminotetrazole

The tetrazole precursor was prepared via a scaled down literature method.<sup>28</sup> 5.78 g (0.055 mol) of cyanogen bromide was dissolved in 100 mL of dried acetonitrile at 0 °C. 15.0 g (0.231 mol) of sodium azide was added to the solution and stirred for 4 hours at 0 °C. In a separate flask, 2.94 g (0.0184 mol) of *O*-benzylhydroxylamine hydrochloride was dissolved in 80 mL of cold distilled water. The aqueous solution was neutralized with 0.73 g (0.0182 mol) of sodium hydroxide and stirred until clear. The acetonitrile cyanogen azide solution was gravity filtered and washed with cold acetonitrile. The filtered inorganic salt was disposed of immediately in a large beaker of alkaline solution. The filtrate was combined with the neutralized *O*-benzylhydroxylamine water solution and stirred for 72 hours and then dried under a stream of air. The crude product was washed with cold water and gravity filtered to yield 2.99 g (0.0156 mol) of 1-benzyloxy-5-aminotetrazole (yield = 85.0%). <sup>1</sup>H NMR (DMSO-*d*<sub>6</sub>): δ = 7.5 (d, 2H, CH-C), 7.4 (t, 2H, CH-CH-C), 7.4 (t, 1H, CH-CH-CH), 7.0 (s, 2H, NH<sub>2</sub>) 5.3 (s, 2H, CH<sub>2</sub>). <sup>13</sup>C NMR (DMSO-*d*<sub>6</sub>): δ = 149.9 (1C, C-NH<sub>2</sub>), 133.3 (1C, C-CH<sub>2</sub>), 130.6 (CH-C), 130.0 (CH-CH-C), 129.0 (CH-CH-CH), 81.4 (1C, CH<sub>2</sub>). <sup>15</sup>N NMR (DMSO-*d*<sub>6</sub>): δ = -6.4 (N-N-N-O), -31.5 (N-N-O), -94.9 (N-N-N-O), -134.8 (N-O), -335.9 (NH<sub>2</sub>). MS (ESI<sup>+</sup>): *m/z* = 192.2 (C<sub>8</sub>N<sub>5</sub>H<sub>9</sub>O<sup>+</sup>).

### 4-benzyloxy-1,5-diaminotetrazolium tosylate (1)

1.91 g (7.44 mmol) of ethyl-*O*-*p*-tolylsulfonfyl-acetohydroximate was stirred in 60% perchloric acid (30 mL) for 2 hours at room temperature. The solution was then poured into ice water. The white aminating agent was extracted from the water using 3 x 25 mL of dichloromethane. The organic layer was dried using magnesium sulphate and filtered. In a separate container, 1.33 g (6.96 mmol) of 1-benzyloxy-5-aminotetrazole was dissolved in 75 mL of acetonitrile and stirred until dissolved. The dichloromethane and acetonitrile solutions were combined and stirred for 18 hours at room temperature. The resultant off-white precipitate was vacuum filtered and allowed to dry to yield 1.12 g (2.96 mmol) of **1**. (yield = 42.5%). TGA: 95 °C (dec.). IR:  $\tilde{\nu}$  = 3313 (w), 3180 (w), 3069 (w), 3031 (w), 2983 (w), 2914 (w), 1726 (m), 1644 (w), 1598 (w), 1496 (w), 1456 (w), 1400 (w), 1392 (w), 1361 (w), 1177 (s), 1187 (s), 1121 (s), 1107 (m), 1034 (s), 1010 (s), 932 (w), 898 (m), 850 (w), 814 (m), 742 (m), 680 (s),

635 (m), 640 (m), 563 (s), 554 (s), 484 (w).  $^1\text{H}$  NMR ( $[\text{D}_6]$ )DMSO):  $\delta$  = 9.5 (s, 2H,  $\text{H}_2\text{N-C}$ ), 7.6 (d, 2H,  $\text{CH-C-CH}_2$ ), 7.4 (t, 2H,  $\text{CH-CH-C-CH}_2$ ), 7.4 (t, 1H,  $\text{CH-CH-CH-C-CH}_2$ ), 7.1 (d, 2H,  $\text{CH-C-CH}_3$ ), 7.2 (d, 2H,  $\text{CH-SO}_3$ ), 7.0 (s, 2H,  $\text{H}_2\text{N-N}$ ), 5.5 (s, 2H,  $-\text{CH}_2$ ), 2.3 (s, 3H,  $-\text{CH}_3$ ).  $^{13}\text{C}$  NMR ( $[\text{D}_6]$ )DMSO):  $\delta$  = 146.0 (1C,  $\text{C-CH}_3$ ), 143.4 (1C,  $\text{C-N}$ ), 138.2 (1C,  $\text{C-CH}_3$ ), 132.4 (1C,  $\text{C-CH}_2$ ), 131.1 (2C,  $\text{CH-C-CH}_2$ ), 130.5 (2C,  $\text{CH-CH-C-CH}_2$ ), 129.2 (1C,  $\text{CH-CH-CH-C}$ ), 128.6 (2C,  $\text{CH-C-CH}_3$ ), 126.0 (2C,  $\text{CH-C-SO}_3$ ), 83.3 (1C,  $\text{CH}_2$ ), 21.2 (1C,  $\text{CH}_3$ ). MS ( $\text{ESI}^+$ ):  $m/z$  = 207.0 ( $\text{C}_8\text{N}_6\text{H}_{12}\text{O}^+$ ), 179.0 ( $\text{C}_8\text{N}_4\text{H}_{12}\text{O}^+$ ); MS ( $\text{ESI}^-$ ):  $m/z$  = 171.1 ( $\text{C}_7\text{H}_7\text{SO}_3^-$ ).  $\text{C}_{15}\text{H}_{18}\text{N}_6\text{O}_4\text{S} \cdot 2[\text{H}_2\text{O}]$  (414.4 g  $\text{mol}^{-1}$ ): calcd. C 43.5%, H 5.4%, N 20.3%; found C 42.8%, H 4.9%, N 20.6%.

#### 4-benzyloxy-1,5-diaminotetrazolium bromide (2)

0.254 g (0.671 mmol) of **1** was dissolved in 15 mL of anhydrous ethanol at room temperature. A molar excess of 48% (w/w) hydrobromic acid was added to the solution and stirred for 10 minutes. The ethanol solution was diluted to 350 mL with diethyl ether. The white precipitate was separated from solution via gravity filtration and dried to yield 0.144 g (0.501 mmol) of **2**. (yield = 74.7%). DSC: 88 °C (dec.). IR:  $\tilde{\nu}$  = 3246 (m), 3202 (m), 3145 (m), 3117 (m), 3044 (m), 1715 (s), 1628 (w), 1566 (m), 1501 (w), 1457 (m), 1400 (m), 1390 (m), 1354 (w), 1331 (w), 1312 (w), 1223 (w), 1181 (w), 1149 (w), 1084 (w), 1029 (w), 1004 (s), 964 (w), 939 (w), 883 (m), 846 (s), 809 (w), 790 (s), 746 (s), 699 (s), 636 (m), 609 (m), 558 (m), 540 (m), 502 (m).  $^1\text{H}$  NMR (DMSO- $d_6$ ):  $\delta$  = 9.5 (s, 2H,  $\text{H}_2\text{N-C}$ ), 7.6 (d, 2H,  $\text{CH-C-CH}_2$ ), 7.5 (t, 2H,  $\text{CH-CH-C}$ ), 7.5 (t, 1H,  $\text{CH-CH-CH-CH}$ ), 7.0 (s, 2H,  $\text{H}_2\text{N-N}$ ), 5.5 (s, 2H,  $-\text{CH}_2$ ).  $^{13}\text{C}$  NMR (DMSO- $d_6$ ):  $\delta$  = 143.4 (1C,  $\text{C-N}$ ), 132.4 (1C,  $\text{C-CH}_2$ ), 131.1 (2C,  $\text{CH-C-CH}_2$ ), 130.5 (2C,  $\text{CH-CH-C-CH}_2$ ), 129.2 (1C,  $\text{CH-CH-CH-C}$ ), 83.3 (1C,  $\text{CH}_2$ ). MS ( $\text{ESI}^+$ ):  $m/z$  207.0 ( $\text{C}_8\text{N}_6\text{H}_{12}\text{O}^+$ ), 179.0 ( $\text{C}_8\text{N}_4\text{H}_{12}\text{O}^+$ ); MS ( $\text{ESI}^-$ ):  $m/z$  = 196.0 ( $\text{CN}_6\text{H}_4\text{OBr}^-$ ).

#### 1,5-diamino-4-hydroxytetrazolium bromide (3)

0.528 g (1.83 mmol) of **2** was dissolved in 40 ml of anhydrous methanol at room temperature. 0.1 g of Pd/C (10%) catalyst was added to the solution and vigorously stirred for 6 hours. A mixture of zinc and 25% (w/w)  $\text{H}_2\text{SO}_4$  solution continuously produced  $\text{H}_2$  gas, which was bubbled through the methanol solution. After stirring, the solution was filtered through Celite<sup>®</sup> and evaporated under a stream of air to yield 0.384 g (1.37 mmol) of crude **3** (crude yield = 74.9%).  $^1\text{H}$  NMR (DMSO- $d_6$ ):  $\delta$  = 8.9 (s, 2H,  $\text{H}_2\text{N-C}$ ), 7.0 (s, 2H,  $\text{H}_2\text{N-N}$ ), 4.0 (s, xH,  $\text{N-OH-Br}$ ).  $^{13}\text{C}$  NMR (DMSO- $d_6$ ):  $\delta$  = 143.0 (1C,  $\text{C-NH}_2$ ). MS ( $\text{ESI}^+$ ):  $m/z$  = 117.1 ( $\text{CN}_6\text{H}_5\text{O}^+$ ), 233.0 ( $\text{C}_2\text{N}_{12}\text{H}_9\text{O}_2^+$ ); MS ( $\text{ESI}^-$ ):  $m/z$  = 196.0 ( $\text{CN}_6\text{H}_4\text{Br}^-$ ).

#### 1,5-diaminotetrazole-4N-oxide (SYX-9)

0.384 g of crude **3** was redissolved in 50 mL of anhydrous ethanol and chilled in an ice bath. The solution was treated with anhydrous 0.0612 M triethylamine in ethanol until the solution reached pH 8. The solution was allowed to sit overnight at 0 °C. Crude greyish-brown **SYX-9** with trace triethylamine precipitated out of solution and was collected by filtration as the evaporation proceeds. The crude solid was washed with 2 x

10 mL of diethylether to yield 0.076 g (0.65 mmol) of pure **SYX-9**. No additional amount of **SYX-9** was isolated from the fully dried ethanol solution. Crystallization was achieved from both evaporation of ethanol under a stream of air and evaporation of DMSO to air (yield from **2** = 35.5%). DSC: 137 °C (dec.), 141 °C (det.). IR:  $\tilde{\nu}$  = 3375 (w), 3318 (w), 3242 (m), 3133 (m), 3050 (m), 2959 (m), 2925 (m), 2851 (m), 1681 (s), 1633 (m), 1583 (w), 1499 (m), 1387 (m), 1364 (m), 1328 (s), 1261 (w), 1233 (w), 1198 (m), 1123 (m), 1019 (s), 961 (s), 917 (m), 820 (s), 794 (s), 705 (m), 651 (m), 636 (m), 614 (s), 584 (s), 409 (s).  $^1\text{H}$  NMR (DMSO- $d_6$ ):  $\delta$  = 7.2 (s, 2H,  $\text{H}_2\text{N-C}$ ), 6.7 (s, 2H,  $\text{H}_2\text{N-N}$ ).  $^{13}\text{C}$  NMR (DMSO- $d_6$ ):  $\delta$  = 139.4 (1C,  $\text{C-NH}_2$ ).  $^{15}\text{N}$  NMR (DMSO- $d_6$ ):  $\delta$  = -28.5 (N-N- $\text{NH}_2$ ), -54.2 (N-N-O), -133.2 (N- $\text{NH}_2$ ), -171.4 (N-O), -306.5 (NH<sub>2</sub>-N), -334.8 (NH<sub>2</sub>-C). MS ( $\text{ESI}^+$ ):  $m/z$  = 117.1 ( $\text{CN}_6\text{H}_5\text{O}^+$ ), 233.0 ( $\text{C}_2\text{N}_{12}\text{H}_9\text{O}_2^+$ ); BAM impact: < 1 J; BAM friction: 30 N.

#### Conflicts of interest

There are no conflicts to declare.

#### Acknowledgements

Financial support of this work by the US Army ACC APG Adelphi Div under grant No. W911NF2020189 "Advancing Army Modernization Priorities through Collaborative Energetic Materials Research; Task 1: CHNOF energetic materials with higher lethality" is acknowledged. The National Science Foundation is acknowledged through the Major Research Instrumentation Program under Grant No. CHE 1625543 for the single crystal X-ray diffractometer. Financial support of our laboratory by Purdue University, The Office of Naval Research (ONR) and the Army Research Office (ARO) is also acknowledged. We thank the Purdue Military Research Initiative for graduate education funding. Lastly, we would like to thank Dr. Stephen Beaudoin for his continual guidance and support.

#### References

- 1 Z. Liu, T. Lu, F. Xue, H. Nie, R. Withers, A. Studer, F. Kremer, N. Narayanan, X. Dong, D. Yu, L. Chen, Y. Liu and G. Wang, *Sci. Adv.*, 2020, **6**, 1–10.
- 2 Y. Tang, D. Kumar and J. M. Shreeve, *J. Am. Chem. Soc.*, 2017, **139**, 13684–13687.
- 3 P. Yin, D. A. Parrish and J. M. Shreeve, *Angew. Chemie - Int. Ed.*, 2014, **53**, 12889–12892.
- 4 M. L. Gettings, M. T. Thoenen, E. F. C. Byrd, J. J. Sabatini, M. Zeller and D. G. Piercey, *Chem. - A Eur. J.*, 2020, **26**, 14530–14535.
- 5 J. R. Yount, M. Zeller, E. F. C. Byrd and D. G. Piercey, *J. Mater. Chem. A*, 2020, **8**, 19337–19347.
- 6 C. Sun, C. Zhang, C. Jiang, C. Yang, Y. Du, Y. Zhao, B. Hu, Z. Zheng and K. O. Christe, *Nat. Commun.*, 2018, **9**, 1–7.
- 7 M. X. Zhang, P. E. Eaton and R. Gilardi, *Angew. Chemie Int. Ed.*, 2000, **39**, 401–404.
- 8 O. T. O'Sullivan and M. J. Zdilla, *Chem. Rev.*, 2020, **120**,

- 5682–5744.
- 9 T. M. Klapötke and D. G. Piercey, *Inorg. Chem.*, 2011, **50**, 2732–2734.
- 10 S. R. Yocca, J. Yount, M. Zeller, E. F. C. Byrd and D. G. Piercey, *Inorg. Chem.*, 2021, **60**, 9645–9652.
- 11 L. Türker, *Def. Technol.*, 2016, **12**, 1–15.
- 12 S. E. Creegan, M. Zeller, E. F. C. Byrd and D. G. Piercey, *Propellants, Explos. Pyrotech.*, 2021, 1–9.
- 13 D. M. Smith, T. D. Manship and D. G. Piercey, *Chempluschem*, 2020, **85**, 2039–2043.
- 14 W. Zhang, T. Zhang, W. Guo, L. Wang, Z. Li and J. Zhang, *J. Energ. Mater.*, 2019, **37**, 433–444.
- 15 S. Inagaki and N. Goto, *J. Am. Chem. Soc.*, 1987, **109**, 3234–3240.
- 16 D. R. Wozniak and D. G. Piercey, *Engineering*, 2020, **6**, 981–991.
- 17 V. A. Tartakovsky, I. E. Filatov, A. M. Churakov, S. L. Ioffe, Y. A. Strelenko, V. S. Kuz'min, G. L. Rusinov and K. I. Pashkevich, *Russ. Chem. Bull.*, 2004, **53**, 2577–2583.
- 18 N. Fischer, D. Fischer, T. M. Klapötke, D. G. Piercey and J. Stierstorfer, *J. Mater. Chem.*, 2012, **22**, 20418–20422.
- 19 I. V. Ovchinnikov, *Dokl. Akad. Nauk.*, 1998, **43**, 67–70.
- 20 P. He, J. Han, J. Wu, H. Mei and J. Zhang, *New J. Chem.*, 2019, **43**, 16454–16460.
- 21 P. Ravi and S. P. Tewari, *Struct. Chem.*, 2012, **23**, 487–498.
- 22 M. Göbel, K. Karaghiosoff, T. M. Klapötke, D. G. Piercey and J. Stierstorfer, *J. Am. Chem. Soc.*, 2010, **132**, 17216–17226.
- 23 T. M. Klapötke, D. G. Piercey and J. Stierstorfer, *Chem. - A Eur. J.*, 2011, **17**, 13068–13077.
- 24 T. Harel and S. Rozen, *J. Org. Chem.*, 2010, **75**, 3141–3143.
- 25 D. E. Chavez, D. A. Parrish, L. Mitchell and G. H. Imler, *Angew. Chemie - Int. Ed.*, 2017, **56**, 3575–3578.
- 26 G.-H. Tao, Y. Guo, D. A. Parrish and J. M. Shreeve, *J. Mater. Chem.*, 2010, **20**, 2999–3005.
- 27 D. G. Piercey, D. E. Chavez, S. Heimsch, C. Kirst, T. M. Klapötke and J. Stierstorfer, *Propellants, Explos. Pyrotech.*, 2015, **40**, 491–497.
- 28 Y. H. Joo, J. H. Chung, S. G. Cho and E. M. Goh, *New J. Chem.*, 2013, **37**, 1180–1188.
- 29 T. M. Klapötke, D. G. Piercey and J. Stierstorfer, *Eur. J. Inorg. Chem.*, 2012, 5694–5700.
- 30 P. N. Gaponik and V. P. Karavai, *Chem. Heterocycl. Compd.*, 1984, **20**, 1388–1391.
- 31 Bruker (2019). Apex3 v2019.1-0, SAINT V8.40A, Bruker AXS Inc.: Madison (WI) USA.
- 32 L. Krause, R. Herbst-Irmer, G. M. Sheldrick and D. Stalke, *J. Appl. Crystallogr.*, 2015, **48**, 3–10.
- 33 SHELXTL suite of programs, Version 6.14, 2000-2003, Bruker Advanced X-ray Solutions, Bruker AXS Inc., Madison, Wisconsin: USA.
- 34 G. M. Sheldrick, *Acta Crystallogr. Sect. A Found. Crystallogr.*, 2008, **64**, 112–122.
- 35 G. M. Sheldrick, *Acta Crystallogr. Sect. C Struct. Chem.*, 2015, **71**, 3–8.
- 36 C. B. Hübschle, G. M. Sheldrick and B. Dittrich, *J. Appl. Crystallogr.*, 2011, **44**, 1281–1284.
- 37 A. Lyakhov, P. Gaponik and S. Voitekhovich, *Acta Crystallogr. Sect. C*, 2001, **C57**, 185–186.
- 38 U. . Nair, S. N. Asthana, A. Subhanandra Roa and B. R. Gandhe, *Def. Sci. J.*, 2010, **60**, 137–151.
- 39 Y. Ji, B. Wang, Z. Zhang, Q. Lu and C. Zhu, *Energ. Mater.*
- 40 A. I. Lesnikovich, O. A. Ivashkevich, S. V. Levchik, A. I. Balabanovich, P. N. Gaponik and A. A. Kulak, *Thermochim. Acta*, 2002, **388**, 233–251.
- 41 WIWEB-Standardarbeitsanweisung 4–5.1.02 Ermittlung der Explosionsgefährlichkeit hier der Schlagempfindlichkeit mit dem Fallhammer Erding.
- 42 W. Häslebarth, *Accredit. Qual. Assur.*, 2002, **7**, 418–419.
- 43 NATO Standardization Agreement (STANAG) on Explosives, Friction, Sensitivity Test, no 4487.
- 44 WIWEB-Standardarbeitsanweisung 4–5.1.03 Ermittlung der Explosionsgefährlichkeit oder der Reibeempfindlichkeit mit dem Reibeapparat Erding, 2002.
- 45 E. F. C. Byrd and B. M. Rice, *J. Phys. Chem. A*, 2006, **110**, 1005–1013.
- 46 B. M. Rice and E. F. C. Byrd, *J. Comput. Chem.*, 2013, **34**, 2146–2151.
- 47 B. M. Rice, J. J. Hare and E. F. C. Byrd, *J. Phys. Chem. A*, 2007, **111**, 10874–10879.
- 48 M. J. Frisch, G. W. Trucks, H. B. Schlegel, G. E. Scuseria, M. A. Robb, J. R. Cheeseman, G. Scalmani, V. Barone, B. Mennucci and G. A. Petersson.
- 49 A. D. Becke, *J. Chem. Phys.*, 1993, **98**, 5648–5652.
- 50 C. Lee, W. Yang and R. G. Parr, *Phys. Rev. B*, 1988, **37**, 785.
- 51 S. H. Vosko, L. Wilk and M. Nusair, *Can. J. Phys.*, 1980, **58**, 1200–1211.
- 52 P. J. Stephens, F. J. Devlin, C. F. Chabalowski and M. J. Frisch, *J. Phys. Chem.*, 1994, **98**, 11623–11627.
- 53 R. Krishnan, J. S. Binkley, R. Seeger and J. A. Pople, *J. Chem. Phys.*, 1980, **72**, 650–654.
- 54 M. J. Frisch, J. A. Pople and J. S. Binkley, *J. Chem. Phys.*, 1984, **80**, 3265–3269.
- 55 P. von Ragué Schleyer, T. Clark, A. J. Kos, G. W. Spitznagel, C. Rohde, D. Arad, K. N. Houk and N. G. Rondan, *J. Am. Chem. Soc.*, 1984, **106**, 6467–6475.
- 56 M. Sućeska, *Mater. Sci. Forum*, 2004, **465–466**, 325–330.
- 57 M. Sućeska, *Propellants, Explos. Pyrotech.*, 1991, **16**, 197–202.
- 58 L. M. Barton, J. T. Edwards, E. C. Johnson, E. J. Bukowski, R. C. Sausa, E. F. C. Byrd, J. A. Orlicki, J. J. Sabatini and P. S. Baran, *J. Am. Chem. Soc.*, 2019, **141**, 12531–12535.
- 59 T. M. Klapötke and M. Sućeska, *Zeitschrift für Anorg. und Allg. Chemie*, 2021, **647**, 572–574.